Humans, Hydrology, and the Distribution of Inorganic Nutrient Loading to the Ocean

STEPHEN V. SMITH, DENNIS P. SWANEY, LIANA TALAUE-McMANUS, JEREMY D. BARTLEY, PEDER T. SANDHEI, CASEY J. McLAUGHLIN, VILMA C. DUPRA, CHRIS J. CROSSLAND, ROBERT W. BUDDEMEIER, BRUCE A. MAXWELL, AND FREDRIK WULFF

Most modern estimates of dissolved nitrogen and phosphorus delivery to the ocean use Meybeck's estimates from approximately 30 large rivers. We have derived an extended database of approximately 165 sites with nutrient loads. For both dissolved inorganic nitrogen (DIN) and dissolved inorganic phosphorus (DIP), the logarithmic yields (log [load/area]) can be parameterized as functions of log (population density) and log (runoff/area) (R^2 for DIN and DIP approximately 0.6). Landscape production of DIN and DIP is largely assimilated. Even though DIN and DIP follow substantially different biogeochemical cycles, loading for DIN and DIP is tightly coupled (R^2 for log DIN versus log DIP approximately 0.8), with a constant loading ratio of about 18:1. Estimates of DIN and DIP fluxes are distributed globally around the world coastlines by using basin population density and runoff at 0.5° increments of latitude and longitude. We estimate that total loads for the 1990s are about three times Meybeck's estimates for the 1970s.

Keywords: global nutrient loads, eutrophication, human influence, rivers

The process of eutrophication represents the biogeochemical response to heavy nutrient loading (Nixon 1995, Cloern 2001). Typical consequences of eutrophication include (a) elevated primary production in response to elevated nutrient delivery and (b) elevated respiration in response to the rapid production of organic matter. In cases of particularly high production and respiration, the sediments or the lower portion of the water column may experience sufficient respiration to strip the water column of oxygen and cause major kills of fish and other organisms. For example, Cooper and Brush (1991) report on the long-term history of anoxia in the Chesapeake Bay, and Welsh and Eller (1991) discuss the phenomenon in Long Island Sound. Periods of anoxia have been documented for portions of numerous North American estuaries (Bricker 1997). Even large areas of the open coastal waters where the Mississippi River discharges nutrient-rich water into the Gulf of Mexico suffer recurrent anoxic events (Rabalais et al. 2002).

While some systems are naturally eutrophic, *cultural* eutrophication represents the special (and increasingly common) case where human activities are responsible for heavy nutrient loading. The Baltic Sea and the Black Sea are two large, well-known systems where human activities have exacerbated a natural tendency towards eutrophic conditions (Larsson et al. 1985, Zaitsev 1991). Eutrophication reflects both natural processes in the catchments draining to the ocean and human modification of nutrient delivery. Hence, an understanding of local, regional, or global patterns of eutrophication requires information on nutrient delivery to the ocean.

Most current estimates of global nutrient delivery to the ocean can be traced to the work of Meybeck (1982). That seminal article presented estimates, nominally for the year 1970, based on approximately 30 rivers. Meybeck estimated that the total dissolved phosphorus (TDP) load to the global ocean in 1970 was 65 x 10^9 moles (mol) per year (yr), of which about 40% (26 x 10^9 mol per yr) was dissolved inorganic phosphorus (DIP). Similarly, he estimated that the total dissolved nitrogen (TDN) delivery to the ocean was 1540 x 10^9 mol per yr, of which about 31% (480 x 10^9 mol per yr) was dissolved inorganic nitrogen (DIN). The flux ratio of DIN to DIP from

Stephen V. Smith (e-mail: svsmith@cicese.mx) was a research professor in the Department of Oceanography at the University of Hawaii when this work was undertaken and is currently an investigator in the Department of Ecology, CICESE (Centro de Investigación Científica y de Educación Superior de Ensenada), Ensenada, Mexico. Dennis P. Swaney is an environmental biologist at the Boyce Thompson Institute, Cornell University, Ithaca, NY 14850. Liana Talaue-McManus is an associate professor in the Division of Marine Affairs, Rosenstiel School of Marine and Atmospheric Science, University of Miami, Miami, FL 33149. Jeremy D. Bartley and Robert W. Buddemeier are research scientists at the Kansas Geological Survey, Lawrence, KS 66047. Peder T. Sandhei and Casey J. McLaughlin are graduate research assistants at the University of Kansas, Lawrence, KS 66047. Vilma C. Dupra is a student at the University of the Philippines Marine Science Institute, Diliman, Philippines. Chris J. Crossland is executive officer at the LOICZ (Land–Ocean Interactions in the Coastal Zone) International Project Office, Netherlands Institute for Sea Research, Texel, The Netherlands. Bruce A. Maxwell is an assistant professor in the Department of Engineering at Swarthmore College, Swarthmore, PA 19081. Fredrik Wulff is a professor of systems ecology at the University of Stockholm, Sweden. © 2003 American Institute of Biological Sciences.

Meybeck's article is approximately 18:1. Although many subsequent modifications of global DIP and DIN flux estimates to the ocean have been made, most, as far as we can see, ultimately trace back to Meybeck's original data.

This article provides a substantially larger and more recent database to refine and update Meybeck's estimate with data primarily from the 1990s. Although the individual river loading estimates are not all of high quality, the pattern is sufficiently robust to provide insight into present spatial distribution of nutrient delivery to the ocean, into possible changes in delivery between 1970 and the 1990s, and into delivery in the absence of significant human influence.

Background and approach for the analysis

The International Geosphere–Biosphere Programme (IGBP) is an international project designed to evaluate the response of the Earth system to global environmental change. Land–Ocean Interactions in the Coastal Zone (LOICZ) is a core project element of IGBP and deals with its mission within the coastal ocean. The IGBP/LOICZ project has developed nutrient budgets for about 200 coastal ecosystems (available at the Biogeochemical Modelling Node on the LOICZ Web site; see box 1) to estimate the biogeochemical fluxes of these materials to the coastal zone and transformations within coastal ecosystems.

These nutrient budgets share the same basic structure, following the LOICZ biogeochemical budgeting guidelines developed by Gordon and colleagues (1996). Estimates of freshwater delivery to individual systems and of water exchange between those systems and the adjacent ocean are established by means of simple box models for water and salt. Dissolved nutrients move with the water and salt from land to the coastal systems and between the coastal systems and the ocean; these nutrients undergo transformations within all of these systems. This simple model structure is widely applicable with minimal data.

Synthesis of the IGBP/LOICZ data is under way. On the basis of results from approximately 200 systems, researchers are developing estimates of the characteristics of nutrient delivery to coastal ecosystems, nutrient processing within those ecosystems, and nutrient exchange with the open ocean. This article represents an important component of that synthesis, dealing with the delivery of nutrients to the coastal zone. Terrigenous loading data derived from the budget sites involves a small number of sites (about 200) scattered along a global coastline with a length on the order of 10^6 kilometers (km).

Coastline length provides a useful scaling function for considering the flux of materials across the boundary between land and ocean. The estimated length is, of course, a function of the scale at which the coastline shape is resolved (Mandelbrot 1967). The length is approximated here at two scales of resolution: (1) Expressed as a simple geometric shape, the length is about 8×10^5 km, estimated as the continental shelf area of about 27×10^6 km^2 (Sverdrup et al. 1942) divided by the average shelf width of about 35 km (extrapolated from Hayes 1964). Geometrically, the world continental shelf can

---

Box 1. Web sites

HYDRO1k Elevation Derivative Database (25 January 2003; *http://edcdaac.usgs.gov/gtopo30/hydro*)

International Geosphere–Biosphere Programme (25 January 2003; *www.igbp.kva.se*)

Kansas Geological Survey: Environmental Database (25 January 2003; *www.kgs.ukans.edu/Hexacoral/Envirodata/envirodata.html*)

Land–Ocean Interactions in the Coastal Zone (LOICZ) International Project Office (25 January 2003; *www.nioz.nl/loicz*)

LandScan: A Global Population Database for Estimating Populations at Risk (25 January 2003; *www.ornl.gov/gist/projects/LandScan/SIMPLE/smaps.htm*)

LOICZ Biogeochemical Modelling Node (25 January 2003; *http://data.ecology.su.se/MNODE*)

National Oceanic and Atmospheric Administration Satellite and Information Services: Shoreline/Coastline Data (25 January 2003; *www.ngdc.noaa.gov/mgg/shorelines/shorelines.html*)

University of New Hampshire/Global Runoff Data Centre Composite Runoff Fields Version 1.0 (25 January 2003; *www.grdc.sr.unh.edu*)

Web-LoiczView Overview (25 January 2003; *www.palantir.swarthmore.edu/loicz/help*)

---

thus be viewed as a long, narrow ribbon, about 20,000 times as long on average as it is wide. (2) The World Vector Shoreline, a digital database at a scale of 1:250,000 that can be searched at the National Oceanic and Atmospheric Administration (NOAA) Web site (box 1; Wessel and Smith 1996), provides a more detailed estimate of coastline length. This estimate resolves most (but not all) coastal embayments budgeted during the LOICZ project and yields a length of about 2×10^6 km.

How can we properly extrapolate the site-specific loading data to a global distribution of nutrient delivery along such a long coastline? To scale upward from the study localities to an estimate of the global distribution pattern of loading, we apply predictions based on analysis of the collective behavior of these systems. As in many earlier studies (Peierls et al. 1991, Howarth et al. 1996, Lewis et al. 1999), we use simple and multiple linear regressions to evaluate relationships between base 10 logarithm ($\log_{10}$)–transformed loads and controlling variables. We also use spatially referenced cluster analysis (Web-LoiczView geospatial clustering, box 1; Maxwell and Buddemeier 2002) to delineate the global distribution of the resulting patterns.

Some budgeted desert systems have no runoff. Small lagoonal or island systems have catchments that are too small to be adequately resolved in global-scale geographic information systems (GIS) data sets. Some systems were excluded from the analysis because data were incomplete or exhibited errors that we have not yet resolved. In addition to the budget sites, this analysis includes 28 river basins for which Meybeck and Ragu (1997) reported inorganic nutrient loads. The analyses used for most of the discussion here are based on 165 systems for which runoff of both DIN and DIP are available.

Our analysis includes two data components. The first component consists of the budget data for specific sites, as described above. The second consists of available environmental data, gridded into 0.5° (latitude/longitude) boxes for the world coastal zone. These data can be found at the Kansas Geological Survey Web site (box 1). The coastal data are for environmental variables corresponding to 0.5° grid cells that contain a portion of the world coastline as defined by the World Vector Shoreline (see NOAA Web site, box 1; Wessel and Smith 1996). Each 0.5° coastal grid cell is connected to a watershed based on a 0.5° stream network, according to data from the Water Systems Analysis Group at the University of New Hampshire (UNH, box 1; Vörösmarty et al. 2000). Runoff data, also at 0.5° resolution from the UNH group, combine observed and modeled runoff. Population estimates (LandScan, box 1; Dobson et al. 2000), originally a 1 km²

resolution data set, were aggregated to each 0.5° grid cell and summed at the basin endpoint—the last cell in the stream network.

Many of the catchments corresponding to the individual budget sites were not well resolved with 0.5° grid data (approximately 2500 km² at the equator). Therefore, a separate data set showing refined catchment data for each watershed was derived using the gridded global elevation database, HYDRO1k (box 1; Verdin and Greenlee 1996), at 1 km² resolution. That is, catchment boundaries were drawn with a resolution of 1 km, using available GIS software (ArcView 3.2). Most catchment basins greater than about 100 km² are apparently adequately resolved. Population data from the LandScan database (box 1; Dobson et al. 2000) were aggregated using the refined basin boundaries. Runoff (V_Q), DIP, and DIN loads are from the budget database (available at the LOICZ Biogeochemical Modelling Node, box 1).

Data distribution

Figure 1 illustrates the basins used and gives some sense of the fraction of the globe that has been included in this analysis. Although the landmass is relatively well represented (about 35% of total land area, a similar percentage of total runoff, and 20% of total population), only a small fraction of the coastal zone is included in the analysis. Designing our analysis around the biogeochemical nutrient budgets for coastal ecosystems (e.g., bays, estuaries, and shelf seas) represents an important
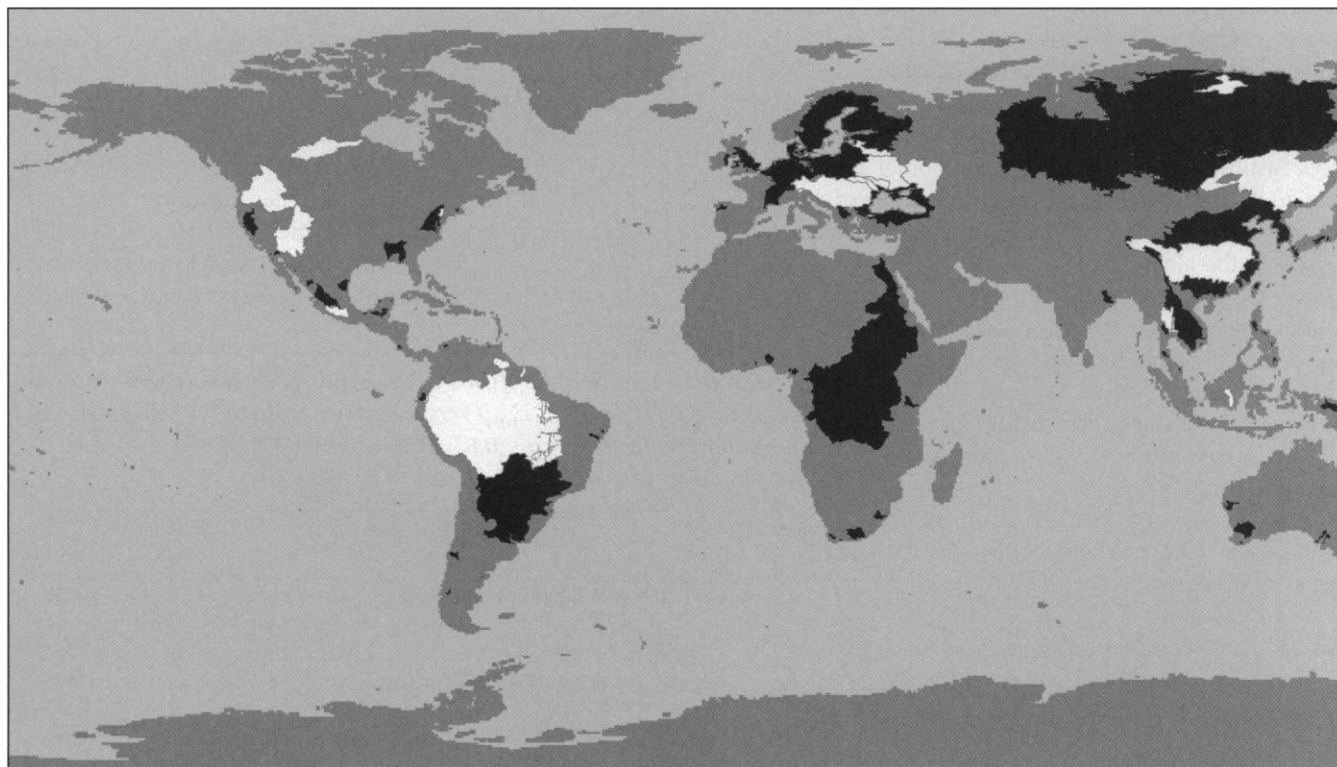

Figure 1. World map showing catchment basins for budget sites from the Land–Ocean Interactions in the Coastal Zone (LOICZ) project (black) and basins from Meybeck and Ragu (1997; white) for which nutrient data are available. The Meybeck and Ragu basins overlap some of the LOICZ basins.

difference from previous studies. In some cases the budget sites are represented by single river systems (e.g., Carmen-Machona Lagoon, Mexico). Other budget sites (e.g., Baltic Sea, North Sea, East China Sea) have numerous rivers delivering materials to the systems.

While large individual river basin catchments are included, many of the catchments are very small watersheds. As a result, the catchment basins used in the analysis vary dramatically in size, from about 10^1 to 10^7 km^2. Catchments smaller than about 10^2 km^2 have poorly resolved basin characteristics, but this only includes six catchment basins used in the analysis. About 60% of the catchments used have areas between 10^3 and 10^5 km^2. The following large ($> 10^6$ km^2) river basins are included: Amazon, Congo, Rio de la Plata, Amur, and Changjiang. These rivers are identified on the scatter diagrams (figures 2, 3).

Characterizing the loads

Nutrient loading from the landscape to the ocean can be broadly separated into two categories of materials: (1) general products of landscape biogeochemical reactions and (2) materials responding to human production. This division is consistent with conclusions drawn by other authors (e.g., Meybeck et al. 1989, Peierls et al. 1991, Howarth et al. 1996, Smith et al. 1997, Seitzinger and Kroeze 1998, Lewis et al. 1999, Seitzinger et al. 2002, van Breeman et al. 2002). Human production incorporates a complex mixture of products, including domestic and industrial sewage, domestic animal waste, fertilizer, and atmospheric fallout from vehicular and industrial nitrogen emissions. Some of these products scale more or less directly to local human population density (e.g., domestic waste discharge); others do not (e.g., agricultural production or atmospheric fallout in areas of low population density). Institutional, socioeconomic, and other aspects of the human dimension locally influence the release of these materials to the environment. In effect, this is the "human footprint" on the global land surface (Sanderson et al. 2002). Water plays a complex role as a transport medium, a reactant in nutrient-related biogeochemical reactions, and a diluent. The coastal zone, and specifically the coastline, is the region where both natural products and products of the human footprint are delivered to the ocean.

It is useful to consider three drivers of nutrient flux: landscape biogeochemistry, human intervention, and runoff. These three drivers cannot be cleanly separated. Runoff interacts with landscape biogeochemistry, and humans affect both the landscape and the hydrologic cycle. We have examined a wide range of basin variables, including area, population, percentage of area covered by roads (as a proxy for human infrastructure), different characterizations of land use, and

temperature- and precipitation-related factors. Only three variables have proved to be strongly related to DIN and DIP loads (L_{DIN} and L_{DIP}, respectively, measured in mol per yr). These variables are (1) runoff (V_Q, measured in cubic meters [m^3] per yr), (2) basin area (A, measured in km^2), and (3) population (N, or number of people; table 1).

We performed our analysis on log_{10}-transformed data. The slope of the log–log relationship between L_{DIN}/A and V_Q/A is 0.81, essentially identical to that (0.84) observed by Lewis and colleagues (1999) for relatively pristine watersheds in the Americas. However, while Lewis and colleagues observed a weaker but significant relationship between L_{DIN}/A and elevation, a similar significant relationship does not appear in our data. The slope of the relationship between log (L_{DIN}/A) and log (N/A) is 0.44. This appears to be intermediate between similar relationships developed for total nitrogen load, or L_{TN} (0.35; Howarth et al. 1996), and for nitrate (NO$_3$) load, or L_{NO_3} (0.53; Peierls et al. 1991); it is essentially the same as for L_{NO_3} in northeastern US watersheds reported by Mayer and colleagues in 2002 (0.47). Temperature shows a complex relationship with nutrient load. In the absence of additional explanatory variables, temperature shows no relationship to L_{DIN} and a negligible effect on L_{DIP}. Combined with the variables N/A and V_Q/A, temperature appears to have a statistically significant negative effect on L_{DIN} but not on L_{DIP} (table 1); in contrast, latitude has no effect.

Some consistent statistical features emerge from the analyses. First of all, L_{DIN} and L_{DIP} are highly correlated (figure 2). Second, pairwise regressions of independent and dependent variables yield slopes fairly near 1 using a model I regression, and slopes statistically equal to 1 based on a model II regression using geometric means (Ricker 1973). This means that all variables, both independent (logarithms of V_Q, A, and N) and dependent (logarithms of L_{DIN} and L_{DIP}), scale directly with basin size. Given these size-dependent regressions, the DIN:DIP loading ratios of large river basins are similar to those of smaller catchments, and the large-basin values cluster near the upper right portion of the regression line. However, the

Table 1. Regression equations for dissolved inorganic phosphorus and dissolved inorganic nitrogen yields (L_{DIP}, L_{DIN}) versus various explanatory variables. All regressions and variables have p < 0.05. The regressions in boldface are the ones used for subsequent analyses.

Dependent variable	Regression equation	Number of sites	R^2
log (L_{DIP}/A)	**2.72 + 0.36 log (N/A) + 0.78 log (V_Q/A)**	165	0.58
log (L_{DIP}/A)	2.13 + 0.47 log (N/A)	174	0.22
log (L_{DIP}/A)	3.23 + 0.88 log (V_Q/A)	165	0.45
log (L_{DIN}/A)	**3.99 + 0.35 log (N/A) + 0.75 log (V_Q/A)**	165	0.59
log (L_{DIN}/A)	3.45 + 0.44 log (N/A)	177	0.22
log (L_{DIN}/A)	4.46 + 0.81 log (V_Q/A)	167	0.40
log (L_{DIN}/A)	4.39 + 0.41 log (N/A) + 0.75 log (V_Q/A) – 0.024 T_{max}	167	0.59

Note: L_{DIN}/A, mol nitrogen per km^2 per yr; L_{DIP}/A, mol phosphorus per km^2 per yr; V_Q/A, m per yr; N/A, people per km^2; T_{max}, maximum monthly average temperature (°C).
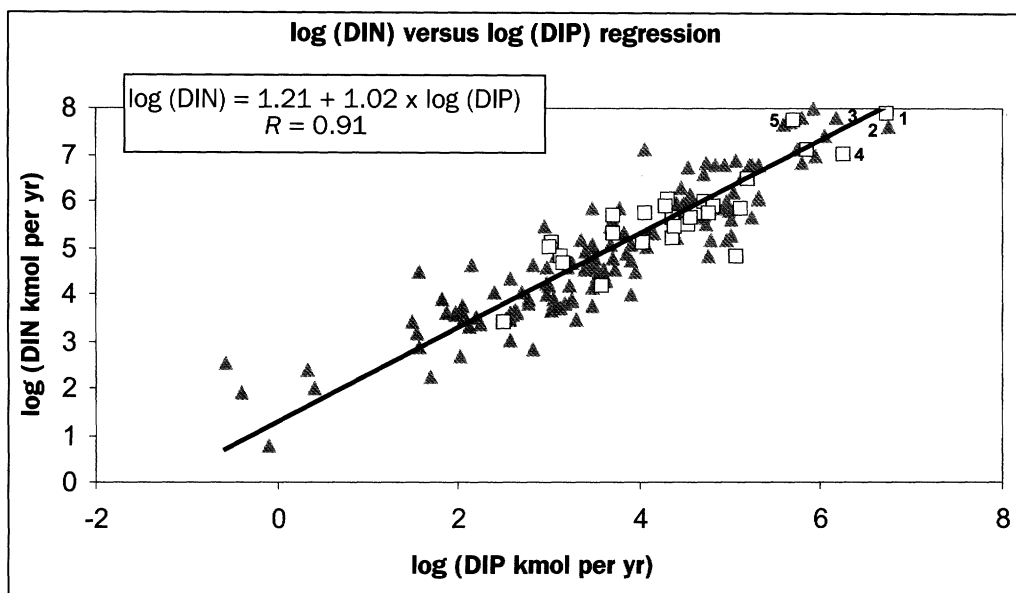
Figure 2. Model II regression line for log dissolved inorganic nitrogen (DIN) versus log dissolved inorganic phosphorus (DIP). Note that slope does not differ significantly from 1. Gray triangles represent Land–Ocean Interactions in the Coastal Zone data; open squares represent data from Meybeck and Ragu (1997). Five large river basins are identified: (1) Amazon, (2) Congo, (3) Rio de la Plata, (4) Amur, and (5) Changjiang.

scatter of data around these size-dependent regressions is large, and simple scale dependence does not provide information about functional relationships among variables.

To identify more useful predictive relationships between nutrient loads and independent variables, we performed exploratory analyses of basin and budget data using stepwise multiple regressions. Equations of the following form work well in scaling the loads to area and predicting both L_{DIP} and L_{DIN} (expressed generically below as L):

$$\log (L/A) = a + b_1 \log (N/A) + b_2 \log (V_Q/A).$$

The original variables (load, number of people, and runoff) are scaled to watershed area to eliminate the simple area dependence described above (figure 3). When the data are normalized by area, the large rivers and Meybeck basins (Meybeck 1982) follow the same trend as the smaller catchments. This parameterization spreads the large systems across the same data range observed in the LOICZ data for smaller systems. The flux per unit area of catchment, called yield, ranges over about four orders of magnitude (from about 1 to more than 10^4 mol per km^2 per yr for L_{DIP}/A; about 20 times these values for L_{DIN}/A). With a few exceptions, data points are within an order of magnitude of the regression lines. Although this represents substantial scatter in the data, the regression relationships contain quite a bit of information.

Surprisingly, the coefficients are virtually identical for L_{DIN} and L_{DIP}, as are the correlations. Both population density and runoff contribute significantly to the equation. This conclusion differs somewhat from that of Peierls and colleagues (1991); they concluded (for NO_3 only) that

water flow and area were not statistically significant independent variables. We think that the inclusion of more small systems in our database has brought out this additional dependence.

Loading scenarios

Useful insight into the equations emerges if they are solved under scenarios of low, intermediate, and high population density, and similarly of low, intermediate, and high runoff (table 2). The intermediate scenario approximates global average conditions, while the high and low scenarios are realistic (but not extreme) conditions. Solutions of the equations have been rearranged in terms of per capita loading and nutrient concentrations, permitting comparison with available information on per capita waste load production and pristine versus polluted water quality. The ranges of both population density and flow examined are well within the bounds of realistic conditions.

At very low population density (N/A = 1 person per km^2) and very low flow ($V_Q/A = 0.01$ m per yr), per capita DIN and DIP fluxes (L_{DIN}/N, L_{DIP}/N) are about 300 and 14 mol per person per yr, respectively. These rates are in the range of estimates from the World Health Organization (WHO; Economopoulos 1993) for per capita domestic waste production (about 300 mol DIN and 30 mol DIP per person per yr). As flow rate rises, per capita loading rises sharply (to about 10,000 and 500 mol DIN and DIP). This runoff-mediated landscape effect probably represents the combined effects of (a) landscape nutrient production under natural conditions and (b) human perturbations that are possible with increased water availability (e.g., agriculture). Because these combined
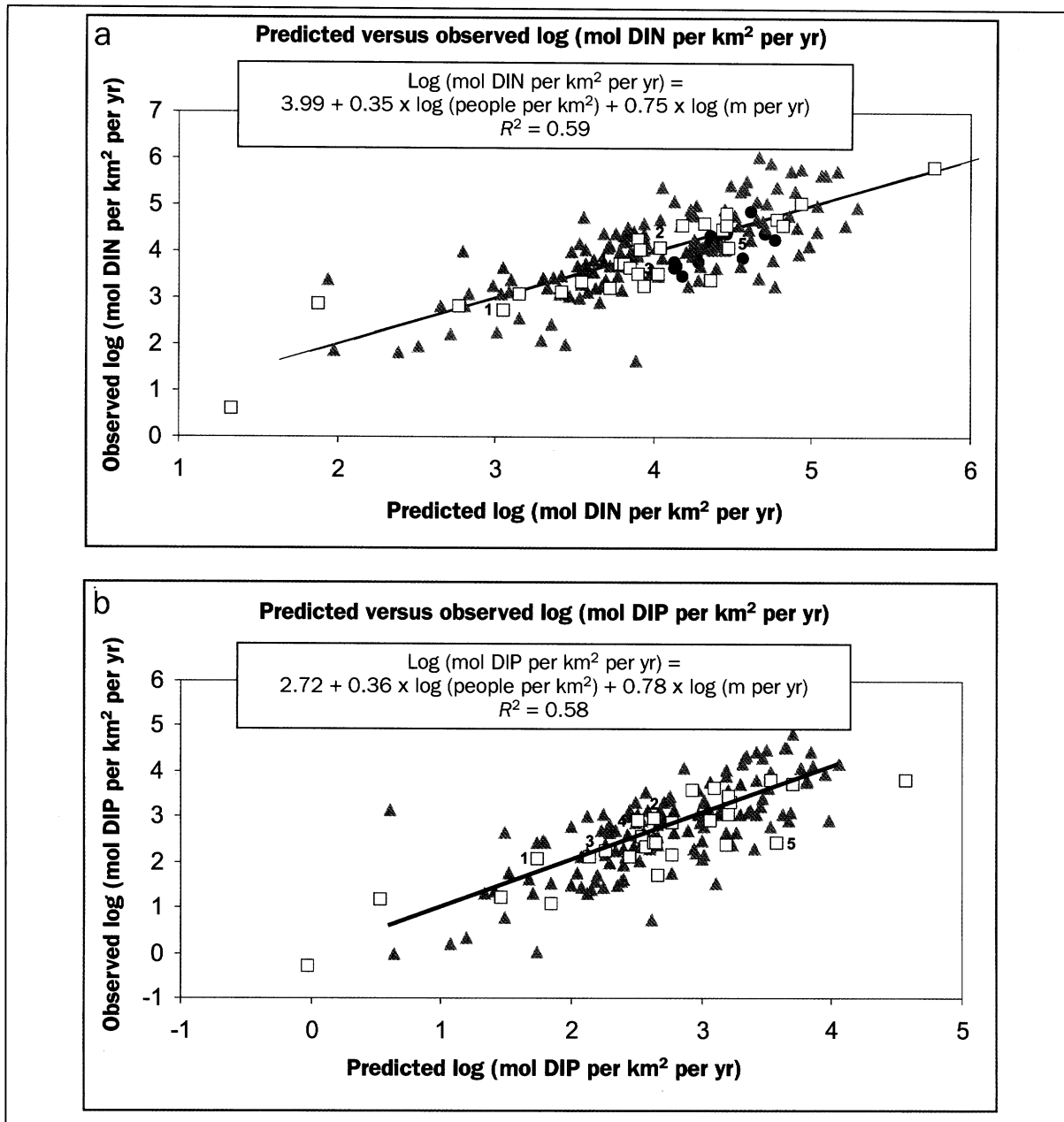
Figure 3. Predicted versus observed values for (a) dissolved inorganic nitrogen (DIN) and (b) dissolved inorganic phosphorus (DIP) loading. Over most of the data range, these equations generate a nitrogen-to-phosphorus molar loading ratio of about 19:1. Gray triangles represent Land–Ocean Interactions in the Coastal Zone data; open squares represent data from Meybeck and Ragu (1997). For DIN, black circles represent NO_3 (nitrate) loads for 16 northeastern US watersheds that were not used in the regression (Boyer et al. 2002, Mayer et al. 2002). Five large river basins are identified: (1) Amazon, (2) Congo, (3) Rio de la Plata, (4) Amur, and (5) Changjiang.

effects are expressed as an increase in per capita load, the load does not necessarily correlate well with population within the catchment.

It is interesting to note the effect of dilution. At low flow conditions, DIN and DIP concentrations (L_{DIN}/V_Q, L_{DIP}/V_Q) are about 30 and 1 millimoles per cubic meter (mmol per m^3), respectively. These measurements are within the range of nutrient concentrations in clean waters (e.g., Meybeck et al.

1989). With high flow and low human population density, the DIN and DIP concentrations become quite low (about 10 and 0.5 mmol per m^3) even though the loads are high. These sorts of concentrations would be typically taken to be "pristine conditions"; the calculations demonstrate the importance of dilution in arriving at these conditions.

Consider the effect of population density. We have seen that at low flow and low population density the per capita fluxes

Table 2. Solution of the dissolved inorganic phosphorus (DIP) and dissolved inorganic nitrogen (DIN) loading equations under scenarios of low and high population density and low and high runoff. The column at far right approximates mean global conditions of population density and runoff.

Variables for scenario development					
Population density (people per km^2)	1 (low)	1 (low)	1000 (high)	1000 (high)	50 (mean)
Runoff (V_Q) per unit area (m per yr)	0.01 (low)	1 (high)	0.01 (low)	1 (high)	0.3 (mean)
Resultant scenario calculations					
DIP yield (mol per km^2 per yr)	14	524	174	6310	839
DIP per capita load (mol per person per yr)	14	524	0.2	6	17
DIP concentration (mmol per m^3)	1.4	0.5	17	6	3
DIN yield (mol per km^2 per yr)	309	9772	3467	109,648	15,577
DIN per capita load (mol per person per yr)	309	9772	3	110	311
DIN concentration (mmol per m^3)	31	10	347	110	52

are fairly close to WHO estimates of domestic waste production. This is probably coincidental; at such low population density it can be assumed that human waste is mostly assimilated within the catchments. At high population density, the per capita loads are well below the WHO estimates. This is consistent with the results of Peierls and colleagues (1991), although they did not note this fact. They concluded that nutrient delivery per catchment area approximated the per capita waste production scaled by catchment area. Their statement cannot be correct over the entire range of the data, because the relationship they derived was based on log–log analysis (as is ours) and the slope of their derived equation was significantly less than unity. Their result was approximately true for the log means of their data set. The population–flux relationship is also approximated in the right column of table 2. Since about half the world population lives in a relatively narrow coastal strip and much of the coastal zone has relatively small catchments, it follows that much of this region will have high nutrient flux per unit area, but low flux per capita.

The tendency to have low per capita load at high population density reflects assimilation or other losses within the catchments. The domestic waste loads represent a low estimate of total human release of nutrients, because there are additional anthropogenic sources (e.g., fertilizer, wastes from animal agriculture, industrial wastes, and atmospheric nitrogen deposition from fossil fuels). The conclusion that per capita nutrient load is relatively low at high population density does not imply that nutrient concentrations are low. At high population density and high runoff, DIP and DIN concentrations are about 6 and 100 mmol per m^3, respectively. These are high (although not extreme) concentrations, reflecting the obvious importance of dilution in ameliorating the effects of pollution sources. The global average scenario (lower

population density and lower flow than the high-density scenario) results in water concentrations within about a factor of two of concentrations obtained from the high-population, high-runoff scenario. At high population and low flow (i.e., low dilution of high human loads), the concentrations climb to about 17 and 350 mmol per m^3, respectively. These would be considered extremely polluted waters.

Biogeochemistry of nitrogen and phosphorus

It is well known that the chemical transformation pathways for nitrogen and phosphorus differ markedly from one another (e.g., Froelich 1988, Schlesinger 1997). In addition to being present in inorganic and organic dissolved forms, nitrogen is involved in biotic reactions and is the primary constituent of the atmosphere. Besides direct uptake and release with respect to organic matter, the biotic processes of nitrogen fixation and denitrification actively move nitrogen between the atmosphere (as nitrogen gas [N_2] and nitrous oxide [N_2O]) and both organic and inorganic forms of fixed nitrogen. Both NO_3 and ammonia (NH_3) are highly soluble in water, and dissolved NH_3 readily ionizes to ammonium (NH_4). NO_3 is an important byproduct of combustion, while NH_3 is a highly volatile byproduct of animal waste. As a result, atmospheric transport and both wet and dry deposition are important pathways by which these materials are delivered to the landscape (e.g., NRC 2000, Meyers et al. 2001). By contrast, phosphorus is involved in biotic reactions, primarily through the relatively simple (though still highly complex) pathways of organic production and oxidation. Phosphorus is also involved in various important mineral reactions (including both precipitation–dissolution of various forms of the mineral group apatite and adsorption–desorption reactions). In general, phosphorus is very particle-reactive and is taken up or released from the particles under changing conditions of pH, redox, and ionic strength. It has no significant gas phase.

The scatter in the loading ratio probably reflects, in large part, the different chemical reaction pathways for DIN and DIP. The only real overlap in the reaction pathways for nitrogen and phosphorus involves production and oxidation of organic matter. Because the composition ratio of nitrogen to phosphorus for most terrestrial organic matter is close to the DIN:DIP loading ratio we observed (approximately 19:1), decomposition of organic matter apparently dominates the inorganic nutrient loading, both in absolute range (figure 3) and loading ratio (figure 2). Mayer and colleagues (2002) have recently suggested on the basis of isotopic analyses that most riverine NO_3 in forested catchments of the northeastern United States originates in soil nitrification processes. In
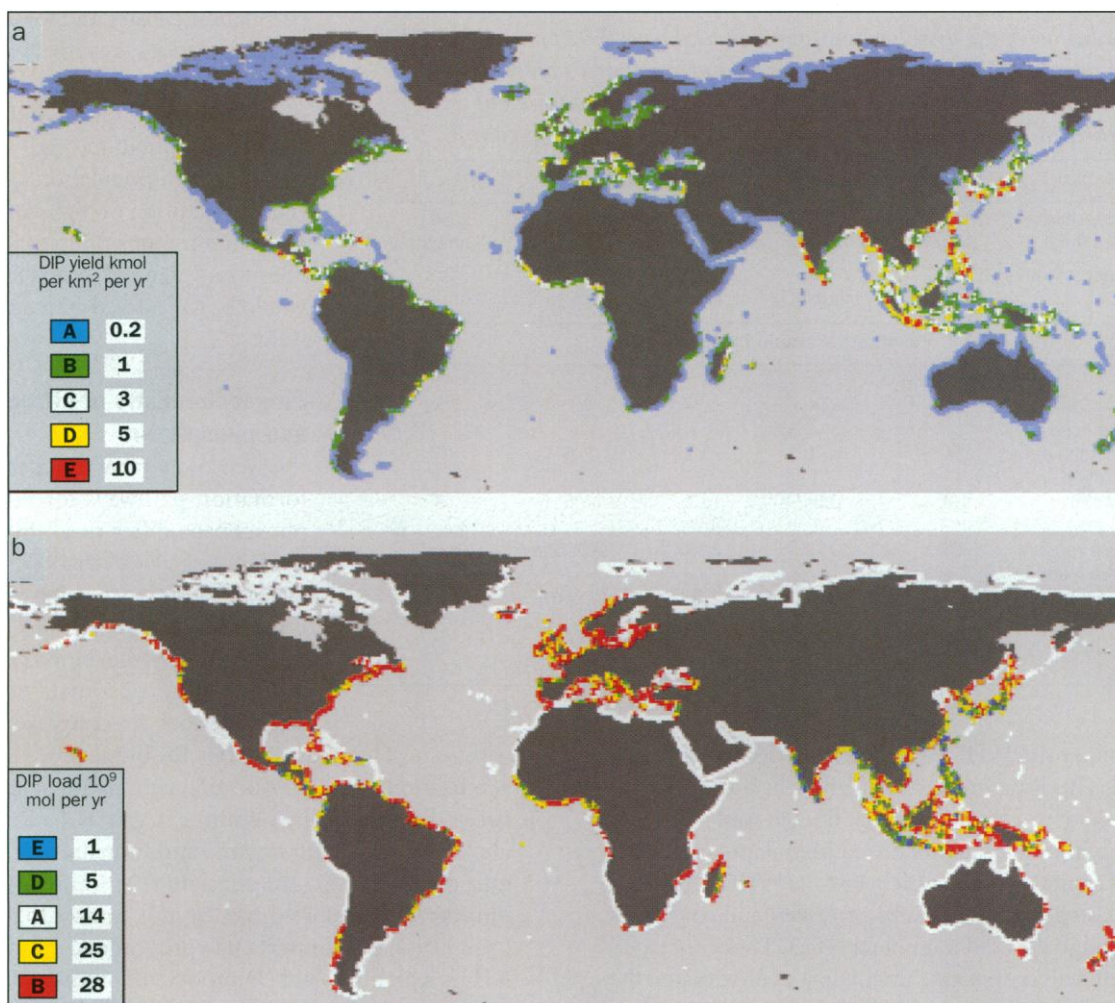
Figure 4. Calculated dissolved inorganic phosphorus (DIP) for the global coastline based on a population–runoff equation. Clusters are identified by the letter in the legend boxes; order is changed by the color-coded ranking in terms of the two variables. (a) DIP yield in kmol per km² per year. The global mean is about 600. (b) DIP load in 10⁹ mol per year.

catchments with significant areas of urban and agricultural land use, wastewater NO_3 is an additional major source and manure a minor source.

The weak but significant temperature effect on nitrogen, but not phosphorus, may reflect the relatively greater biotic control on reactions within the nitrogen cycle. The fact that the temperature–nitrogen correlation is negative might suggest, for example, that the temperature signal represents the dependence of denitrification on temperature (Knowles 1981). We had expected that, as in previous studies (e.g., Boyer et al. 2002), land use, as well as land area, might explain a significant part of the variation in nutrient loading. Apparently any such effects are largely assimilated within the effects of area, population, and runoff as we have parameterized them, at least at this scale.

Global distribution patterns of yields and loads

Interesting questions arise in extrapolating from the estimated loads per area of the sites used here to estimates for the global coastal zone. There are at least three different ways one might scale the data: (1) yield (L/A, the direct output of the regression models in figure 3; this might be viewed as a hydrological characterization of the catchment function); (2) total load (L, a measure of delivery to the ocean); and (3) load relative to the area of the receiving water body. This third category might be viewed as a measure of impact on the receiving water body, allowing for system volume and exchange rate (both of which further scale the load by dilution). The load and yield analyses are presented below; impact analyses are still under development.

The master regression equations (L_{DIP}/A and L_{DIN}/A as functions of V_Q/A and N/A) were solved using land area, population, and runoff for the basin connected to each of the 0.5° coastal cells (i.e., data in 0.5° grids containing shoreline, as described above) to describe yield for those basins. Once the yield estimates were derived, cluster analysis (Maxwell and Buddemeier 2002) was used to group these cells into classes based on similarity between the

estimated DIP yields for the basins (arithmetic rather than log-transformed DIP yields were used in the clustering). Five clusters of DIP yields were derived (figure 4a). After the initial clustering, the individual clusters were evaluated for their mean DIP and DIN yields and total loads (figure 4b). The cluster data were color coded according to the rank of the mean yields for each cluster; the same color code ranking was then used to rank the clusters according to their summed load contribution to the ocean. DIP yields for the clusters vary between 0.2 and 10 kilomoles (kmol) per km^2 per yr, while DIP loads for the clusters vary between 1×10^9 and 28×10^9 mol per yr.

The two clusters that contribute over 70% of the total load (clusters B and C) have low to intermediate yields (1 and 3 kmol DIP per km^2 per yr, respectively). These clusters include mostly temperate or tropical regions with high runoff, including large rivers. Conversely, the cluster with the highest yield (cluster E, with 10 kmol per km^2 per yr), which includes mostly coastal areas in Asia and a few in Latin America, has the lowest global load (about 1%), because the extreme-yield sites tend to represent a small number of relatively small basins. This finding indicates that highly polluted systems, while important to nutrient conditions of local receiving waters, are relatively less significant than the larger number of less polluted systems in terms of the global river transport of these dissolved inorganic nutrients to the ocean.

Load contributions vary from the relatively small contribution of 1×10^9 mol per yr (cluster E) to 28×10^9 (cluster B). The average global yield of DIP to the ocean according to this analysis is about 0.6 kmol per km per yr; the total global load (table 3) is estimated as 74×10^9 mol per yr. This load is almost three times the value of 26×10^9 mol per yr derived by Meybeck (1982). For DIN, a similar cluster analysis gives the same global distribution of clusters, with a global load of 1350 $\times 10^9$ mol per yr, also about three times the value of 480×10^9 mol per yr reported by Meybeck (1982). The DIN:DIP loading ratio that we derive (18:1) is close to the ratio he reported.

We believe these figures constitute the first revision of Meybeck's (1982) estimates, based on a substantially larger database than he had. Although we cannot rule out the possibility that part of this difference is due to the difference between Meybeck's expert judgment of how to extrapolate his data globally and our statistical (but not necessarily better) extrapolation of a larger data set, the direction and general magnitude of change in loading seems reasonable. Our results are consistent with changes that would be expected from

Table 3. Summary of cluster statistics for dissolved inorganic phosphorus and dissolved inorganic nitrogen loads to the global coastal zone. See figure 4 for comparison. (Cluster sums may not match the global load because of rounding.)

Cluster	Phosphorus load (10^9 mol per yr)	Nitrogen load (10^9 mol per yr)	Number (%) of coastal cells	
Red (B)	28	525	1395	(20)
Yellow (C)	25	447	615	(9)
White (A)	14	269	4852	(68)
Green (D)	5	83	210	(2)
Blue (E)	1	16	44	(1)
Global load (total)	74	1350	7116	(100)

Table 4. Summary of cluster statistics for dissolved inorganic phosphorus and dissolved inorganic nitrogen yields to the global coastal zone. See figure 4 for comparison.

Cluster	Phosphorus yield (kmol per km^2 per yr)	Nitrogen yield (kmol per km^2 per yr)	Number (%) of coastal cells	
Red (E)	10	170	44	(1)
Yellow (D)	5	85	210	(2)
White (C)	3	47	615	(9)
Green (B)	1	17	1395	(20)
Blue (A)	0.2	4	4852	(68)
Global yield (total)	0.6	12	7116	(100)

two decades of population growth and land-use change (see also Mackenzie et al. 2000).

Finally, we consider various estimates of nutrient transport under natural conditions. Meybeck (1982) estimated the natural DIP load to be about 13×10^9 mol per yr and the DIN load to be 320×10^9 mol per yr. These loads can be compared with our results in several ways.

If we assume that the low-yield cluster of our analysis (cluster A; 0.2 kmol DIP per km^2 per yr) approximates natural loading, we can extrapolate this loading globally. This cluster accounts for a load of about 14×10^9 mol per yr, about 19% of the total load. It also accounts for about 68% of the number of coastal cells (tables 3, 4). We infer that pristine loading might be the cluster A loading divided by 0.68, or about 21×10^9 mol per yr. This value is approximately 30% of the present DIP load to the world oceans. As an alternative extrapolation, we substitute population densities of 0.1 and 1 person per km^2 for each one of the catchments draining the coastal grid cells while retaining the runoff from those cells. This yields load estimates of 10×10^9 and 23×10^9 mol DIP per yr, respectively. Similar analysis for DIN load gives 400×10^9 mol per yr based on cluster A, and 180×10^9 to 400×10^9 mol per yr based on the two population density estimates.

While these extrapolations are inevitably rough, they give some indication of the degree of human modification of global nutrient loads and are in remarkable agreement with Meybeck's estimates. Apparently human activities have increased DIP and DIN loading above natural fluxes by more than a factor of three, and those changes appear to be recognizable on time scales as short as two decades.

Summary and conclusions

In the process of using a global data set that is largely independent of the widely used Meybeck data set, we have derived global loading estimates that are higher than his estimates for two decades earlier. We developed regressions to describe nutrient loading for 165 sites worldwide, together with the geospatial clustering tool Web-LoiczView, to make estimates of the global distribution patterns of load and yield as functions of population density and runoff.

While some of the difference between Meybeck's results and ours could reflect our more extensive data set and different method of extrapolating from specific sites to the global coastal zone, we suspect that much of the difference is real. Total human population, plant and animal agricultural production, and atmospheric nitrogen emissions have all increased dramatically between the 1970s and the 1990s; it is therefore likely that nutrient loads have increased as well. Further, both Meybeck's estimates and ours demonstrate substantially lower and internally consistent values for natural fluxes of inorganic nutrients to the ocean.

Finally, we call attention to the remarkable correlation between DIP and DIN flux, and the virtually identical forms of their respective prediction equations. This correlation exists despite ample evidence that most of the local production of DIP and DIN does not reach the ocean, and despite the very different chemical transformation pathways for these two nutrients.

References cited

Boyer EW, Goodale CL, Jaworski NA, Howarth RW. 2002. Anthropogenic nitrogen sources and relationships to riverine nitrogen export in the northeastern U.S.A. Biogeochemistry 57–58: 137–169.

Bricker S. 1997. NOAA's National Estuarine Eutrophication Survey: Selected results for the Mid-Atlantic, South Atlantic and Gulf of Mexico regions. Estuarine Research Federation Newsletter 23: 20–21.

Cloern JE. 2001. Our evolving conceptual model of the coastal eutrophication problem. Marine Ecology Progress Series 210: 223–253.

Cooper SR, Brush GS. 1991. Long-term history of Chesapeake Bay anoxia. Science 254: 992–996.

Dobson JE, Bright EA, Coleman PR, Durfee RC, Worley BA. 2000. A global population database for estimating population at risk. Photogrammetric Engineering and Remote Sensing 66: 849–858.

Economopoulos AP. 1993. Assessment of Sources of Air, Water, and Land Pollution: A Guide to Rapid Source Inventory Techniques and Their Use in Formulating Environmental Control Strategies. Geneva (Switzerland): World Health Organization.

Froelich PN. 1988. Kinetic control of dissolved phosphate in natural rivers and estuaries: A primer on the phosphate buffer mechanism. Limnology and Oceanography 33: 649–668.

Gordon DC, Boudreau PR, Mann KH, Ong J-E, Silvert W, Smith SV, Wattayakorn G, Wulff T, Yanagi T. 1996. LOICZ Biogeochemical Modelling Guidelines. Den Burg (The Netherlands): LOICZ Reports and Studies no. 5.

Hayes MO. 1964. Lognormal distribution of inner continental shelf widths and slopes. Deep-Sea Research 11: 53–78.

Howarth RW, et al. 1996. Regional nitrogen budgets and riverine N and P fluxes for the drainages to the North Atlantic Ocean: Natural and human influences. Biogeochemistry 35: 75–79.

Knowles R. 1981. Denitrification. Pages 315–329 in Clark FE, Rosswall T, eds. Terrestrial Nitrogen Cycles. Stockholm: Swedish Natural Science Research Council. Ecological Bulletins no. 33.

Larsson UR, Elmgren R, Wulff F. 1985. Eutrophication and the Baltic Sea: Causes and consequences. Ambio 14: 9–14.

Lewis WM Jr, Melack JM, McDowell WH, McClain M, Richey JE. 1999. Nitrogen yields from undisturbed watersheds in the Americas. Biogeochemistry 46: 149–162.

Mackenzie FT, Ver LM, Lerman A. 2000. Coastal-zone biogeochemical dynamics under global warming. International Geology Review 42: 193–206.

Mandelbrot B. 1967. How long is the coast of Britain? Statistical self-similarity and fractal dimension. Science 156: 636–638.

Maxwell BA, Buddemeier RW. 2002. Coastal typology development with heterogeneous data sets. Regional Environmental Change 3: 77–87.

Mayer B, et al. 2002. Sources of nitrate in rivers draining sixteen watersheds in the northeastern U.S.: Isotopic constraints. Biogeochemistry 57–58: 171–197.

Meybeck M. 1982. Carbon, nitrogen, and phosphorus transport by world rivers. American Journal of Science 282: 401–450.

Meybeck M, Ragu A, eds. 1997. River Discharges to the Oceans: An Assessment of Suspended Solids, Major Ions, and Nutrients. Environmental and Assessment Document. Nairobi (Kenya): United Nations Environment Programme.

Meybeck M, Chapman DV, Helmer R, eds. 1989. Global Freshwater Quality: A First Assessment. Oxford (United Kingdom): Blackwell Reference.

Meyers T, Sickles J, Dennis R, Russell RK, Galloway J, Church T. 2001. Atmospheric nitrogen deposition to coastal estuaries and their watersheds. Pages 53–76 in Valigura RA, Alexander RB, Castro MS, Meyers TP, Paerl HW, Stacey PE, Turner RE, eds. Nitrogen Loading in Coastal Water Bodies: An Atmospheric Perspective. Washington (DC): American Geophysical Union.

Nixon SW. 1995. Coastal marine eutrophication: A definition, social causes, and future concerns. Ophelia: 41: 199–219.

[NRC] National Research Council. 2000. Clean Coastal Waters. Washington (DC): National Academy Press.

Peierls B, Caraco N, Pace M, Cole J. 1991. Human influence on river nitrogen. Nature 350: 386–387.

Rabalais NN, Turner RE, Scavia D. 2002. Beyond science and into policy: Gulf of Mexico hypoxia and the Mississippi River. BioScience 52: 129–142.

Ricker WE. 1973. Linear regressions in fishery research. Journal of the Fisheries Research Board of Canada 30: 409–434.

Sanderson EW, Malanding J, Levy MA, Redford KH, Wannebo AV, Woolmer G. 2002. The human footprint and the last of the wild. BioScience 52: 891–904.

Schlesinger WH. 1997. Biogeochemistry: An Analysis of Global Change. 2nd ed. San Diego: Academic Press.

Seitzinger SP, Kroeze C. 1998. Global distribution of nitrous oxide production and N inputs in freshwater and coastal marine ecosystems. Global Biogeochemical Cycles 12: 93–113.

Seitzinger SP, Styles RV, Boyer EW, Alexander RB, Billen G, Howarth R, Mayer B, van Breemen N. 2002. Nitrogen retention in rivers: Model development and application to watersheds in the northeastern U.S.A. Biogeochemistry 57–58: 199–237.

Smith RA, Schwarz GE, Alexander RB. 1997. Regional interpretation of water-quality monitoring data. Water Resources Research 33: 2781–2798.

Sverdrup HU, Johnson MW, Fleming RH. 1942. The Oceans. Englewood Cliffs (NJ): Prentice-Hall.

van Breeman N, et al. 2002. Where did all the nitrogen go? Fate of nitrogen inputs to large watersheds in the northeastern U.S.A. Biogeochemistry 57–58: 267–293.

Verdin KL, Greenlee SK. 1996. Development of continental scale digital elevation models and extraction of hydrographic features. In Proceedings, Third International Conference/Workshop on Integrating GIS and Environmental Modeling; 21–26 January 1996; Santa Fe, New Mexico.

Vörösmarty CJ, Fekete BM, Meybeck M, Lammers RB. 2000. Global system of rivers: Its role in organizing continental land mass and defining land-to-ocean linkages. Global Biogeochemical Cycles 14: 599–621.

Welsh BL, Eller FC. 1991. Mechanisms controlling summertime oxygen depletion in western Long Island Sound. Estuaries 14: 265–278.

Wessel P, Smith WHF. 1996. A global self-consistent, hierarchical, high-resolution shoreline database. Journal of Geophysical Research 101: 8741–8743.

Zaitsev YP. 1991. Cultural eutrophication of the Black Sea and other European seas. La Mer 29: 1–7.